

Interaction acoustic waves with a layered structure containing layer of bubbly liquid

Damir Gubaidullin^{1,*}, Anatolii Nikiforov¹

¹Institute of Mechanics and Engineering, Kazan Science Center, Russian Academy of Sciences, 420111 Kazan, Russia

Abstract. The results of a theoretical study of the effect of a bubble layer on the propagation of acoustic waves through a thin three-layered barrier at various angles of incidence are presented. The barrier consists of a layer of gel with polydisperse air bubbles bounded by layers of polycarbonate. It is shown that the presence of polydisperse air bubbles in the gel layer significantly changes the transmission and reflection of the acoustic signal when it interacts with such an obstacle for frequencies close to the resonant frequency of natural oscillations of the bubbles. The frequency range is identified where the angle of incidence has little effect on the reflection and transmission coefficients of acoustic waves.

1 Introduction

Gas bubbles are the most acoustically active, natural and widespread formations in the liquid. The presence of a small amount of bubbles significantly increases the compressibility of the medium, while the density of the medium remains close to the density of the liquid. In addition, the oscillating bubble medium has strong dissipative properties, the resulting dissipative losses are mainly associated with interfacial heat transfer. Such special properties of bubble liquids make it possible to use bubble screens as ultrathin anti-hydrolocation coatings [1]. At present, air bubble layers are already being used to shield noise from anthropogenic activities during underwater drilling operations, noise from vibrations of other technical devices, and pile driving in coastal zones [2]. Acoustic properties of the near-bottom bubble layers are actively studied, including in the case of an oblique incidence of an acoustic wave [3]. The main aspects of the mechanics and thermophysics of bubbles and bubble liquids are presented in [4-6]. Various results of theoretical and experimental studies of the dynamics of acoustic waves in bubble media, including media containing bubble layers, are presented in [7-18]. Experimental work [11] presents the results of distortion of an acoustic signal when it falls along the normal to a flat sample consisting of two layers of polycarbonate and a layer containing an industrial gel with polydisperse bubbles.

In this paper we investigate the effect of a bubble layer on the passage of an acoustic signal through a three-layered barrier at various angles of incidence.

2 Theory

The present analysis is based on a dispersion relation which is well established in the case of propagation of

pressure pulses of the small amplitude through the multilayer sample containing a layer of liquid with polydisperse gas bubbles (e.g.[9,12])

$$\left(\frac{K_*}{\omega}\right)^2 = \frac{1}{C_f^2} + \frac{3\alpha_{g0}\alpha_{l0}\rho_{l0}\langle Q \rangle}{3\gamma_g p_{l0} - \langle QS \rangle}, \quad (1)$$

$$C_f = C_l / \alpha_{l0}, \quad S = i\omega a^2 h_a \rho_{l0} / (1 + h_a t_a),$$

$$h_a = -i\omega + 4\nu_l / a^2, \quad t_a = a / (C_l (\alpha_{g0})^\beta), \quad \beta = \frac{1}{6},$$

$$Q = 1 + 3(\gamma_g - 1)[y \cdot \coth(y) - 1] / y^2, \quad y = \sqrt{-i\omega a^2 / \kappa_g},$$

$$\langle Q \rangle = \frac{1}{\rho_g} \int_{a_{\min}}^{a_{\max}} N(a) g(a) Q da, \quad \rho_g = \int_{a_{\min}}^{a_{\max}} N(a) g(a) da,$$

$$\langle QS \rangle = \frac{1}{\rho_g} \int_{a_{\min}}^{a_{\max}} N(a) g(a) QS da, \quad g(a) = \frac{4}{3} \pi a^3 \rho_g$$

in which ρ_{l0} , p_{l0} are the density and pressure of the unperturbed liquid, α_{g0} is the bubble volume content ($\alpha_{l0} = 1 - \alpha_{g0}$), C_l the speed of sound in liquid, ν_l the coefficient of the kinematic viscosity of liquid, ρ_{g0} the density of the gas in bubbles, γ_g the adiabatic index of the gas in bubbles, $N(a)$ the distribution function of bubbles over the radii a ($a_{\min} \leq a \leq a_{\max}$), κ_g the coefficient of thermal diffusivity of the gas, and c_p the specific heat capacity of the gas in bubbles at constant pressure. This dependence of the wave number $K_* = K_{**} + iK$ on the frequency ω allows us to determine the attenuation coefficient K and the phase velocity $C_p = \omega / K_{**}$.

* Corresponding author: damirgubaidullin@gmail.com

According to [8], the size distribution function $N(a)$ is determined as

$$N(a) = \frac{n_t}{\sqrt{2\pi\varepsilon}} \exp\left(-\frac{(\ln(a/a_0))^2}{2\varepsilon^2}\right) \quad (2)$$

in which $a_0 = 0.08$ mm, $\varepsilon = 0.06$, $n_t = 50$ are the distribution parameters [8].

The pulse perturbation of the pressure is given using the imaginary part of the Morlet wavelet with the spike frequency ω_s

$$p'(0, t) = \text{Im}\left(\exp(-i2\pi\omega_s(t-\tau)) \exp\left(\frac{-(t-\tau)^2}{2\delta^2}\right)\right) \quad (3)$$

Parameter τ determines the location, and δ is the spike width.

The fast Fourier transform (FFT) method is used for the calculation of the dynamics of small-amplitude pulse perturbations. In accordance with the representation of the Fourier analysis, the arbitrary spatial-temporal pulse can be written in the form of the following integral:

$$y(x, t) = \int_{-\infty}^{\infty} Y(\omega) \exp[i(K_*x - \omega t)] d\omega \quad (4)$$

This relation determines the inverse Fourier transform of the spectral function $Y(\omega)$. The function $Y(\omega)$ is found from the given initial signal

$$Y(\omega) = \frac{1}{2\pi} \int_{-\infty}^{\infty} y(0, t) \exp(i\omega t) dt \quad (5)$$

This relation determines the direct transform, the function $y(0, t)$.

The methods of the discrete Fourier transform are used for the numerical calculation of the dynamics of pulse pressure perturbation p' . Pulse p' is presented in the form of the finite sum of harmonic waves

$$p'(x, t) = \sum_{m=0}^{L-1} z_m \exp[i(K_*(\omega_m)x - \omega_m t)] \quad (6)$$

$$p'(0, t) = \sum_{m=0}^{L-1} z_m \exp(i\omega_m t) \quad (7)$$

In accordance with (5) for the determination of $p'(x, t)$, it is necessary to find coefficients z_m and the relation (6) should be fulfilled. FFT algorithms were used to find coefficients z_m and to determine $p'(x, t)$. Expanding the initial pulse into the discrete Fourier series and summing its harmonic components in the new position, it is possible to obtain the transformed pulse formed under the action of the dispersion and dissipation.

The following calculation technique is used for the calculation of the interaction of the acoustic signal in water with the multilayer object containing a layer of the bubbly liquid. According to [13], the result of the passage of the plane monochromatic wave $\sim \exp(iKx - \omega t)$ through the multilayer object is plane wave $\sim W \exp(iKx - \omega t)$ where W is the transmission coefficient of the wave, which is determined in terms of impedances of layers Z_i and input impedances of

boundaries of layers Z_i^{in} . For a multilayer object consisting of n layers, the transmission coefficient W and the reflection coefficient R have the form

$$W = \frac{2Z_1}{Z_1 + Z_2} \prod_{j=2}^n \left(\frac{Z_j^{in} + Z_j}{Z_j^{in} + Z_{j+1}} \exp(iK_j d_j \cos \theta_j) \right) \quad (8)$$

$$R = \frac{Z_n^{in} - Z_{n+1}}{Z_n^{in} + Z_{n+1}} \quad (9)$$

$$Z_j = \rho_j \frac{\omega}{K_j \cos \theta_j},$$

$$Z_j^{in} = \rho_j \frac{Z_{j-1}^{in} - iZ_j \text{tg}(K_j d_j \cos \theta_j)}{Z_j - iZ_{j-1}^{in} \text{tg}(K_j d_j \cos \theta_j)} Z_j, \quad Z_1^{in} = Z_1,$$

in which d_j , K_j are the thickness and wave number of the j -th layer, θ_j is the angle formed by the direction of propagation of the wave in the layer with the normal to the boundaries of the layer. The wave number for a layer with a bubble liquid is determined using the dispersion relation (1).

3 Results

The calculations were carried out for a multilayered media, as shown in Fig. 1. Similarly to [8], a multilayered object consisting of two identical layers of polycarbonate of a thickness of $d_2 = d_4 = 1.6$ mm a layer between which ($d_3 = 1$ mm) is filled with a gel with air bubbles is used. This object is placed into a water between a source of the acoustic signal (piezoelectric transducer) and a hydrophone.

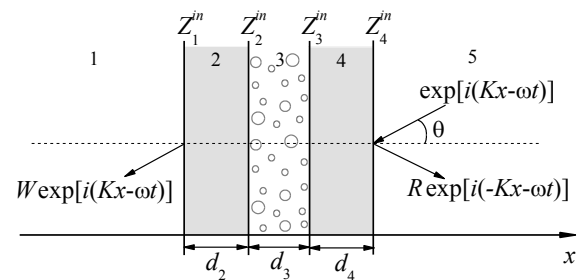


Fig. 1. Multilayered media scheme.

Using the inverse Fourier transform, the complex amplitudes of the harmonic components of the initial pressure pulse $p'(0, t)$ are calculated, where the boundary between media 5 (water) and layer 4 is taken as the position $x=0$. Then, the amplitudes of the harmonic components of the pulse passing through the obstacle to the media 1 (water) are determined, i.e. in water ($x = d_2 + d_3 + d_4$). The change in pressure as a function of time in the new position is calculated using a direct Fourier transform.

In Fig. 2 and Fig. 3 show the results of the calculation of the dependences of the reflection coefficient modulus and the transmission coefficient

modulus on the dimensionless frequency f/f_M ($f = \omega/2\pi$), where f_M is the Minnaert resonant frequency

$$f_M = \frac{1}{2\pi a_0} \sqrt{\frac{3\gamma_g p_0}{\rho_{l0}^{\circ}}} \quad (10)$$

The radius a_0 is a parameter of the distribution function used (2). For the given conditions, $f_M = 40.8$ kHz. The calculations are performed both for a three-layer barrier containing a bubble gel layer (curves *I* and *II*) and for a barrier containing a bubble-free gel layer, i.e. at $\alpha_g = 0$ (curves *III* and *IV*). Accordingly, curves *I* and *III* are calculated at $\theta = 0$, *II* and *IV* – at $\theta = \pi/6$.

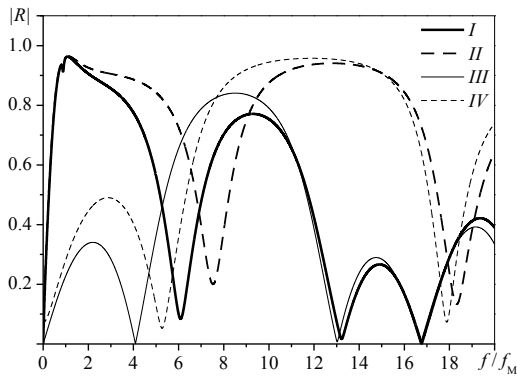


Fig. 2. Dependence of the reflection coefficient modulus on the dimensionless frequency.

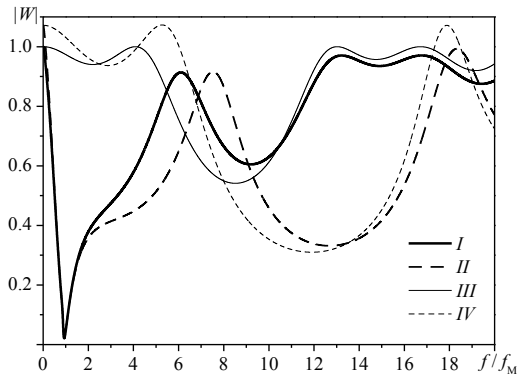


Fig. 3. Dependence of the transmission coefficient modulus on the dimensionless frequency.

The dependence R on Fig. 2 is largely determined by the effects of interference of waves reflected on individual boundaries [13]. It is not difficult to calculate that the minima of curve *III* in Fig. 2 correspond to frequencies determined by the relations previously obtained in [14]

$$f\left(\frac{d_P}{C_P} + \frac{d_l}{C_l}\right) = \frac{1}{4}n, \quad (n=1,3,5,\dots) \quad (11)$$

$$f\left(\frac{d_l}{C_l}\right) = \frac{1}{2}n, \quad (n=1,2,3,\dots) \quad (12)$$

Here, the subscript P denotes the parameters of the polycarbonate layer ($d_P = d_2 = d_4$), the subscript l denotes the parameters of the bubble-free gel.

For curves *I* and *II* in Fig. 2 and Fig. 3, i.e. when there are air bubbles in the gel, a significant difference from curves *III* and *IV*, when there are no bubbles in the gel, is achieved in the frequency range $f/f_M < 5$. This range includes two frequency-domain regions characteristic of the bubble medium—the low-frequency region and the band of acoustic opacity [4, 11]. In the low-frequency region ($f \leq f_M$), the effect of the sound dispersion is determined by interphase temperature nonequilibrium and the value of the phase velocity is much smaller C_l . In the band of acoustic opacity

$$(f_M < f < f_C, \quad f_C = f_M \sqrt{1 + \frac{\rho_{l0}^{\circ} \alpha_g C_l^2}{\gamma_g p_0}} \approx 5f_M), \quad \text{the}$$

values of the phase velocity and the attenuation coefficient assume anomalously high values. For frequencies $2 < f/f_M < 5$ the influence of the angle of incidence is weak, the character of the curves $|R|$ and $|W|$ varies little. For frequencies $f/f_M < 2$ curves *I* and *II* practically do not differ, i.e. in this frequency range the effect of the angle of incidence on $|R|$ and $|W|$ is not essential. The minimum $|W|$ and maximum $|R|$ are reached in the region of the resonance frequency of the bubbles ($f/f_M = 1$), i.e. there is almost complete reflection ($|R| \approx 0.95$). For frequencies $f/f_M > 5$, the phase velocity C_p in a gel with bubbles tends to its asymptotic value – the frozen velocity of sound $C_f = C_l/\alpha_l$ which differs little from the speed of sound in a pure gel [4]. Reduced density of bubble gel $\rho = \rho_l + \rho_g = \rho_l^{\circ} \alpha_l + \rho_g^{\circ} \alpha_g \approx \rho_l^{\circ} \alpha_l \approx \rho_l^{\circ}$. Thus, for high frequencies $f/f_M > 5$, the acoustic properties of the bubble gel layer and the bubble-free gel layer differ little.

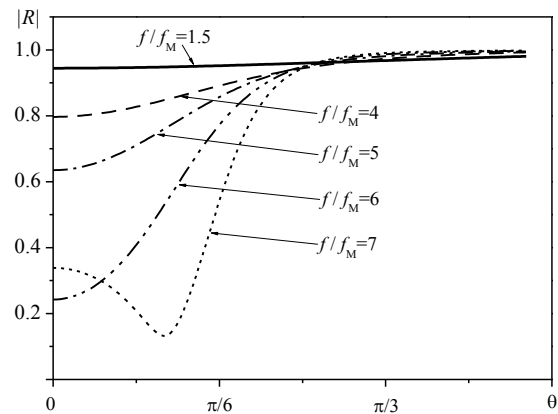


Fig. 4. The angular dependence of the reflection coefficient modulus on the barrier at various dimensionless frequencies.

In Fig. 4 and Fig. 5, the dependences of the modules of the coefficients of reflection and transmission of

acoustic waves are plotted against the angle of incidence.

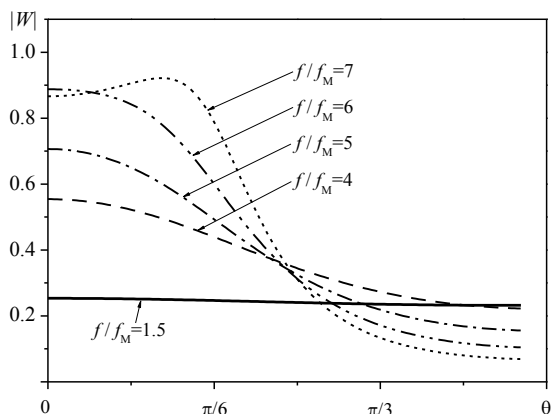


Fig. 5. The angular dependence of the transmission coefficient modulus on the barrier at various dimensionless frequencies.

As noted above, for frequencies $f/f_M < 2$ the influence of the angle of incidence on $|R|$ and $|W|$ is practically absent. In the frequency range $2 < f/f_M < 5$ the value of the angle of incidence already has some effect on $|R|$ and $|W|$ but the curves still remain monotonic. For frequencies $f/f_M > 5$ where the effect of bubbles in the gel on the acoustic properties of the layer does not appear, the angular dependences $|R|$ and $|W|$ become nonmonotonic. But such a character of the curves $|R|$ and $|W|$ is determined only by the laws of reflection and transmission of waves in a multilayer media [13] and will differ little from the form of the curves calculated for the object with a layer of bubble-free gel.

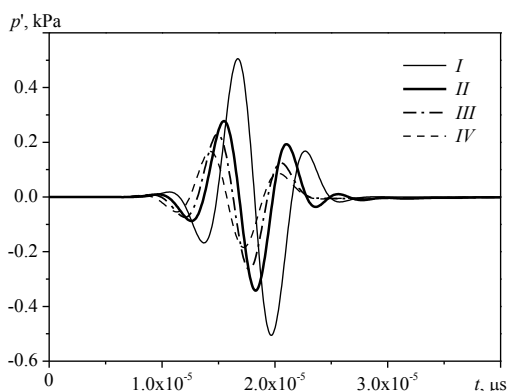


Fig. 6. Pulsed pressure perturbation in water containing a multilayered object.

The form of the pressure pulse after its passage through the three-layer object at various angles of incidence onto the obstacle is shown in Fig. 6, and in Fig. 7 shows the corresponding dimensionless amplitude spectrum of the Fourier transform. The number of harmonics of the FFT subroutine is selected from the motion condition of the pulse in the purified water (when there is no object) without distortion. Lines *I* – the initial pressure pulse (3), lines *II*, *III* and *IV* are calculated for

the transmitted signal at $\theta = 0$, $\theta = \pi/6$ and $\theta = \pi/4$, respectively.

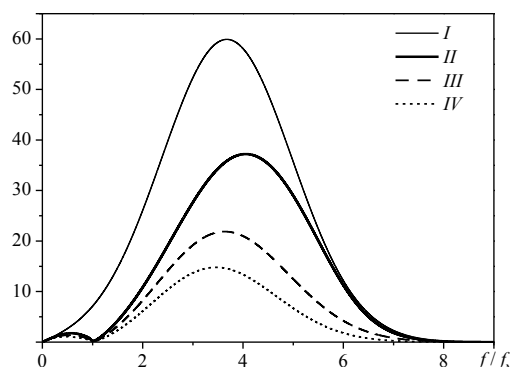


Fig. 7. Amplitude spectrum of Fourier transform.

As the angle of incidence increases, the attenuation of the pulse passing through the object increases. The main carrier frequency (the spike frequency) of the considered pulse is $f_s = 0.15$ MHz ($f_s/f_M = 3.8$). If we compare curves *II-IV* in Fig. 6 and the corresponding amplitude spectra in Fig. 7, it is obvious that the amplitude of the low-frequency harmonics ($f/f_M < 2$) with a change in the slope angle remains practically unchanged. However, the original signal is set in such a way that the major part of its harmonics is in the frequency region $2 < f/f_M < 5$. This determined the dependence of the attenuation of the transmitted pressure pulse on the angle of incidence. Attenuation of the pressure passing through the object, whose amplitude spectrum will be in the frequency range $f/f_M < 2$ will not depend on the angle of incidence. For a pressure pulse whose amplitude spectrum will be in the frequency range $f/f_M > 5$ the effect of bubbles in the gel layer will not appear.

4 Conclusions

The interaction of a small-amplitude pressure pulse with a thin three-layer object at various angles of incidence is theoretically studied. It is shown that the presence of polydispersed air bubbles in the gel layer substantially changes the transmission and reflection of acoustic waves for frequencies less than or close to the resonance frequency oscillations of the bubbles with characteristic mean radius of the bubble size distribution function and for frequencies of the acoustic opacity band. A range of frequencies less than the doubled resonant frequency is revealed, where the dependence of the transmission of acoustic waves through an three-layer object on the angle of incidence is not significant. In this frequency range, the transmission and reflection of acoustic waves will be influenced by the dimensions of the bubbles, their volume content and their thermophysical properties.

The study was performed by a grant from the Russian Science Foundation (project No. 15-11-20022).

References

1. V. Leroy, A. Strybulevych, M. Lanoy, F. Lemoult, A. Tourin, J.H. Page, *Phys. Rev. B.* **91**, 2, 020301 (2015)
2. B. Würsig, C.R. Jr. Greene, T.A. Jefferson, *Mar. Environ. Res.* **49**, 1, 79-93 (2000)
3. V.A. Gusev, O.V. Rudenko, *Acoust. Phys.* **61**, 2, 152-164 (2015)
4. R.I. Nigmatulin, *Dynamics of Multiphase Media* (Hemisphere, New York, 1990)
5. S. Temkin, *Suspension Acoustics: An Introduction to the Physics of Suspensions* (Cambridge Univ. Press, New York, 2005)
6. T.G. Leighton, *The Acoustic Bubble* (Academic, London, 1994)
7. D.A. Gubaidullin, A.A. Nikiforov, *High Temp.* **48**, 2, 170–175 (2010)
8. V. Leroy, A. Strybulevych, J.H. Page, M.G. Scanlon, *J. Acoust. Soc. Am.* **123**, 4, 1931–1940 (2008)
9. D.A. Gubaidullin, Yu.V. Fedorov, *J. Appl. Math. Mech.* **77**, 5, 532-540 (2013)
10. R.I. Nigmatulin, D.A. Gubaidullin, A.A. Nikiforov, *Dokl. Phys.* **59**, 6, 286–288 (2014)
11. V.Sh. Shagapov, V.V. Sarapulova, *Acoust. Phys.* **61**, 1, 37-44 (2015)
12. D.A. Gubaidullin, A.A. Nikiforov, *High Temp.* **55**, 1, 95–100 (2017)
13. L.M. Brekhovskikh, *Waves in Layered Media* (Academic, New York, 1976)
14. D.L. Folds, C.D. Loggins, *J. Acoust. Soc. Am.* **62**, 5, 1102–1109 (1977)